

# An Anisotropic Phong Light Reflection Model

Michael Ashikhmin      Peter Shirley  
University of Utah  
www.cs.utah.edu

## Abstract.

We present a new BRDF model that attempts to combine the advantages of the various empirical models currently in use. In particular, it has intuitive parameters, is anisotropic, energy-conserving, reciprocal, has an appropriate non-Lambertian diffuse term, and is well-suited for use in a Monte Carlo framework.

## 1 Introduction

Physically-based rendering systems describe reflection behavior using the *bidirectional reflectance distribution function* (BRDF) [3]. At a given point on a surface the BRDF is a function of two directions, one toward the light and one toward the viewer. The characteristics of the BRDF will determine what “type” of material the viewer thinks the displayed object is composed of, so the choice of BRDF model and its parameters is important.

We would like to have a BRDF model that works for “common” surfaces such as metal and plastic, and has the following characteristics:

1. **Plausible:** as defined by Lewis [6], this refers to the BRDF obeying energy conservation and reciprocity.
2. **Anisotropy:** the material should model simple anisotropy such as seen on brushed metals.
3. **Intuitive parameters:** for material such as plastics there should be parameters such as  $R_d$  for the substrate and  $R_s$  for the normal specular reflectance as well as two roughness parameters  $n_u$  and  $n_v$ .
4. **Fresnel behavior:** specularity should increase as the incident angle goes down.
5. **Non-Lambertian diffuse term:** The material should allow for a diffuse term, but the component should be non-Lambertian to assure energy conservation in the presence of Fresnel behavior.
6. **Monte Carlo friendliness:** there should be some reasonable probability density function that allows straightforward Monte Carlo sample generation for the BRDF.

Neumann et al’s metallic model [7] captures items 1, 3, 4, and 6. Schlick’s model [9] captures items 2, 3, and 4. Ward’s model [11] captures items 2, and 3. It only violates item 1 for energy conservation at grazing angles. It also approximates Monte Carlo friendliness by giving a sample generation method but does not specify what the underlying density function is, so unbiased sampling is not feasible. Lafortune’s model [5] captures some of these items, but it is not really intended for use with hand-set parameters.

Our goal is to find a BRDF with all the properties outlined. Our basic strategy is to make a Fresnel-weighted Phong-style cosine lobe model that is anisotropic. This strategy borrows pieces from Ward’s model [11] and from Neumann and Neumann’s

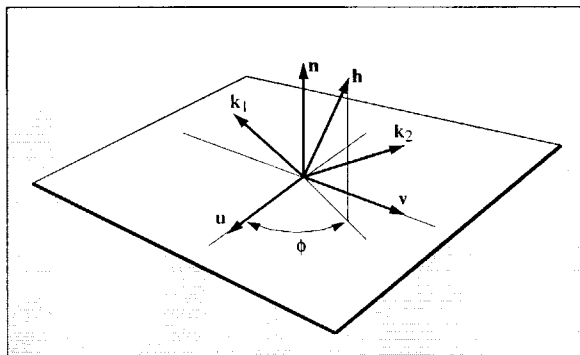


**Fig. 1.** Geometry of reflection. Note that  $\mathbf{k}_1$ ,  $\mathbf{k}_2$ , and  $\mathbf{h}$  share a plane, which usually does not include  $\mathbf{n}$ .

$(\mathbf{a}\mathbf{b})$	scalar (dot) product of vectors $\mathbf{a}$ and $\mathbf{b}$
$\mathbf{k}_1$	normalized vector to light
$\mathbf{k}_2$	normalized vector to viewer
$\mathbf{n}$	surface normal to macroscopic surface
$\rho(\mathbf{k}_1, \mathbf{k}_2)$	BRDF
$\mathbf{h}$	normalized half-vector between $\mathbf{k}_1$ and $\mathbf{k}_2$
$p_h(\mathbf{h})$	probability density function for half-vector
$p(\mathbf{k})$	probability density function for reflection sampling rays
$F(\cos \theta)$	Fresnel reflectance for incident angle $\theta$

**Table 1.** Important terms used in the paper

model [7]. In addition, we add some correction terms that are crucial to keep the directional hemispherical reflection near the desired level. For the diffuse term we use the basic method of Shirley et al. [10] to allow the diffuse-specular tradeoff to conserve energy.

We decompose the BRDF into a specular component and a diffuse component. Accordingly, we write our BRDF as the classical sum of two parts:

$$\rho(\mathbf{k}_1, \mathbf{k}_2) = \rho_s(\mathbf{k}_1, \mathbf{k}_2) + \rho_d(\mathbf{k}_1, \mathbf{k}_2), \quad (1)$$

where the first term accounts for the specular reflection and will be presented in the next section. While it is possible to use the Lambertian BRDF as diffuse term  $\rho_d(\mathbf{k}_1, \mathbf{k}_2)$  in our model, we will discuss a better solution in section 3. We discuss how to implement the model in Section 4. Readers who just want to implement the model should skip to that section.

## 2 Anisotropic specular BRDF

Several shapes for the specular lobe have been proposed with Phong power-of-cosine lobe being the most popular. This is primarily due to its simplicity. The original form of the Phong shader [8] has several problems which triggered the development of more physically plausible Phong-style BRDFs [4, 6, 7]. We will also use a Phong-style specular lobe in our model but will make this lobe anisotropic and incorporate Fresnel be-

havior while attempting to preserve the simplicity of the initial model and physical plausibility achieved earlier for the Phong BRDF by other researchers.

As our starting point we will choose recent result of Neumann and Neumann [7] who improved energy conservation properties of Phong model and made the BRDF well-suited for importance sampling in a Monte Carlo framework. Their main result in our notation is:

$$\rho(\mathbf{k}_1, \mathbf{k}_2) = c * \frac{(\mathbf{r}_1 \mathbf{k}_2)^n}{\max((\mathbf{n} \mathbf{k}_1), (\mathbf{n} \mathbf{k}_2))} F(\cos \theta), \quad (2)$$

where  $n$  is Phong exponent,  $\mathbf{r}_1$  is the unit vector in the direction of mirror reflection of vector  $\mathbf{k}_1$  around the surface normal,  $c$  is a normalization constant and  $F(\cos \theta)$  is the Fresnel fraction. Several choices of argument  $\theta$  are discussed by the authors. The division by  $\max((\mathbf{n} \mathbf{k}_1), (\mathbf{n} \mathbf{k}_2))$  ‘‘pumps up’’ the total hemispherical reflectance  $R(\mathbf{k})$  of the surface and in the limit  $n \rightarrow \infty$  (Phong representation of a perfect mirror) gives  $R(\mathbf{k}) = 1$  for any  $\mathbf{k}$  not exactly at grazing incidence. While there are several ways to achieve this behavior, this particular form preserves reciprocity and avoids the divergence near the grazing angle frequently observed for other simple models.

To extend this model to anisotropic surfaces we use an approach similar to Ward’s [11] who made the parameters of his gaussian lobe model depend on the azimuthal angle of the unit half vector with respect to a system of coordinates attached to the surface. Instead of single Phong parameter  $n$  in Equation 2 we introduce two parameters  $n_u$  and  $n_v$  and write the exponent as  $n_u \cos^2 \phi + n_v \sin^2 \phi$  where  $\phi$  is the azimuthal angle of half-vector  $\mathbf{h}$ . To get better intuition about the model and, more importantly, to allow more efficient importance sampling of the specular lobe in a way discussed below, we also replace the Phong cosine  $(\mathbf{r}_1 \mathbf{k}_2)$  by  $(\mathbf{n} \mathbf{h})$ , a transformation originally proposed by Blinn [1]. Our BRDF is now

$$\rho(\mathbf{k}_1, \mathbf{k}_2) = c * \frac{(\mathbf{n} \mathbf{h})^{n_u \cos^2 \phi + n_v \sin^2 \phi}}{\max((\mathbf{n} \mathbf{k}_1), (\mathbf{n} \mathbf{k}_2))} F(\cos \theta). \quad (3)$$

Although our model is mostly empirical, to proceed further it is useful to interpret certain parts of Equation 3 in terms of physics-based microfacet models [2]. These models treat a surface as a collection of small mirror-like facets. Reflection from these facets is is governed by Fresnel laws. At a high level, a BRDF obtained with such models have the form

$$\rho(\mathbf{k}_1, \mathbf{k}_2) = c * p_h(\mathbf{h}) \text{Vis}(\mathbf{k}_1, \mathbf{k}_2, \mathbf{h}) F((\mathbf{h} \mathbf{k})), \quad (4)$$

where  $p_h(\mathbf{h})$  is the microfacet probability density function,  $F$  is the Fresnel fraction and  $\text{Vis}$  is the microfacet visibility function which gives the probability for a given microfacet to be visible from both directions  $\mathbf{k}_1$  and  $\mathbf{k}_2$  and accounts for most of the complexity of a given microfacet model. Visibility function is also responsible for ensuring the energy conservation. We will not attempt to find a direct analog of this complicated  $\text{Vis}$  function in our empirical model and will be simply concerned with providing the means to conserve energy. However, other terms of Equation 4 do have direct counterparts in Equation 3. For example, it is immediately clear that the appropriate choice for the argument of the Fresnel fraction  $F$  is  $(\mathbf{h} \mathbf{k})$ . Note that throughout the paper we will drop the subscript of vector  $\mathbf{k}$  if either  $\mathbf{k}_1$  or  $\mathbf{k}_2$  can be used. We will also introduce notation

$$p_h(\mathbf{h}) = \frac{\sqrt{(n_u + 1)(n_v + 1)}}{2\pi} (\mathbf{n} \mathbf{h})^{n_u \cos^2 \phi + n_v \sin^2 \phi}, \quad (5)$$

where the normalization constant is chosen so that  $p(\mathbf{h})$  is a true probability density function (integrates to one over the hemisphere of possible  $\mathbf{h}$  directions). Energy conservation requirement can be written as

$$R(\mathbf{k}_1) = \int_{\mathbf{k}_2} \rho(\mathbf{k}_1, \mathbf{k}_2) (\mathbf{k}_2 \mathbf{n}) d\omega_{\mathbf{k}_2} \leq 1 \quad (6)$$

for any  $\mathbf{k}_1$ . Division by  $\max((\mathbf{n}\mathbf{k}_1), (\mathbf{n}\mathbf{k}_2))$  in our model will be cancelled (or replaced by a number less than 1) by  $(\mathbf{n}\mathbf{k}_2)$  factor and we obtain the condition

$$c' * \int_{\mathbf{k}_2} p_h(\mathbf{h}) F((\mathbf{h}\mathbf{k})) d\omega_{\mathbf{k}_2} \leq 1 \quad (7)$$

The assumption of mirror reflection from microfacets gives an important relationship between differential solid angles in the space of reflected rays and the  $\mathbf{h}$ -space of microfacet normal directions [2]:

$$d\omega_{\mathbf{k}_2} = 4(\mathbf{k}_1 \mathbf{h}) d\omega_{\mathbf{h}}. \quad (8)$$

Using this formula and the fact that  $F \leq 1$  we obtain

$$c' * \int_{\mathbf{h}} p_h(\mathbf{h}) 4(\mathbf{k}_1 \mathbf{h}) d\omega_{\mathbf{h}} \leq 1. \quad (9)$$

The integration is now done over a complex subregion of  $\mathbf{h}$ -space. However, being conservative, we can extend the integral over the whole hemisphere of directions. This formula shows that if we divide our BRDF by  $4(\mathbf{k}\mathbf{h})$  and set  $c' = 1$  we will guarantee that our model will conserve energy since  $p_h(\mathbf{h})$  integrates to one over the hemisphere. Putting all this together, we arrive at the final form of our anisotropic specular BRDF:

$$\rho(\mathbf{k}_1, \mathbf{k}_2) = \frac{\sqrt{(n_u + 1)(n_v + 1)}}{8\pi} \frac{(\mathbf{n}\mathbf{h})^{n_u \cos^2 \phi + n_v \sin^2 \phi}}{(\mathbf{h}\mathbf{k}) \max((\mathbf{n}\mathbf{k}_1), (\mathbf{n}\mathbf{k}_2))} F((\mathbf{k}\mathbf{h})) \quad (10)$$

In our implementation we use Schlick's approximation to Fresnel fraction [9]:

$$F((\mathbf{k}\mathbf{h})) = R_s + (1 - R_s)(1 - (\mathbf{k}\mathbf{h}))^5, \quad (11)$$

where  $R_s$  is material's reflectance for the normal incidence.

As a visualization of the energy normalization of the model, we rendered a variety of spheres with different parameters shown in Figure 2. The spheres are in a "furnace" with radiance one in all directions. Perfectly reflecting spheres, regardless of BRDF, would also be white. Essentially it is a visualization of the directional hemispherical reflectance (directional albedo) for a variety of input angles.

The specular BRDF 10 described in this section is useful for representing metallic surfaces where the diffuse component of reflection is very small. Figure 3 shows a set of golden spheres on a texture-mapped Lambertian plane. As the values of parameters  $n_u$  and  $n_v$  change, the appearance of the spheres shift from rough metal to almost perfect mirror, and from highly anisotropic to the more familiar phong-like behavior.

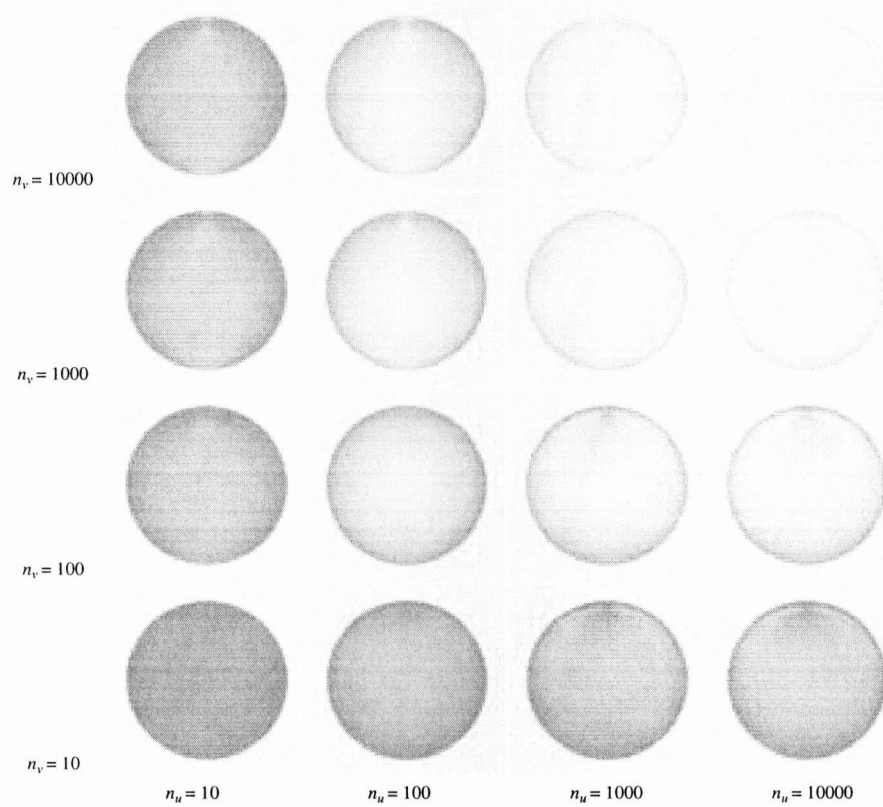


**Fig. 2.** Spheres in a furnace. As the exponents get larger, less energy is "lost". For the center of the darkest sphere,  $n_u = n_v = 10$ , the luminance is about 68% of the background luminance.

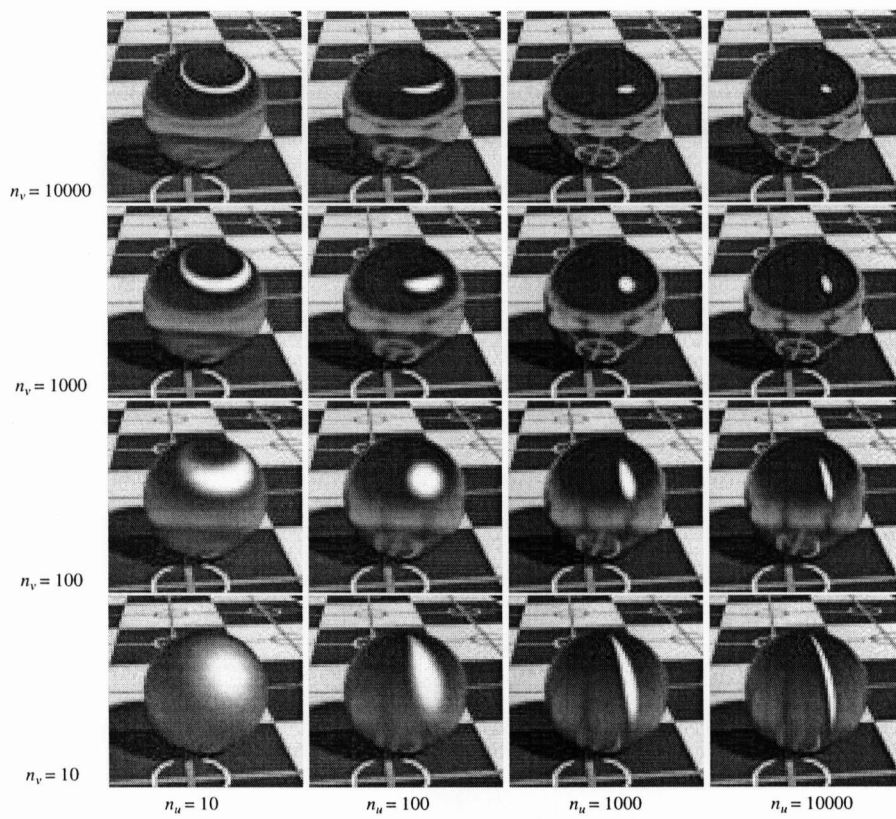


**Fig. 3.** *Metallic spheres for various exponents.*

### 3 Diffuse term

It is possible to use a Lambertian BRDF together with our specular term in a way this is done for most models [9, 11]. However, we derive a simple angle-dependent form of the diffuse component accounts for the fact that the amount of energy available for diffuse scattering varies due to the dependence of specular term's total reflectance on the incident angle. In particular, diffuse color of a surface disappears near the grazing angle because the total specular reflectance is close to one in this case. This well-known effect cannot be reproduced with a Lambertian diffuse term and is therefore missed by most reflection models. Another, perhaps more important, limitation of the Lambertian diffuse term is that it must be set to zero to ensure energy conservation in the presence of a Fresnel-weighted term.

Shirley et al. [10] proposed a simple form of a non-Lambertian diffuse BRDF which takes this issue into account while preserving overall energy conservation and reciprocity. We use this result in the following form:

$$\rho_d(\mathbf{k}_1, \mathbf{k}_2) = c * R_d(1 - R(\mathbf{k}_1))(1 - R(\mathbf{k}_2)), \quad (12)$$

where  $R(\mathbf{k})$  is the total hemispherical reflectance of the specular term as defined by equation 6,  $0 < R_d < 1$  is the diffuse albedo of the surface and  $c$  is a normalization constant computed such that for  $R_d = 1$  the total incident and reflected energies are the same.

For this form to be directly used in our model, we need a closed-form expression for  $R(\mathbf{k})$ . Unfortunately, specular BRDF (Equation 10) does not allow for the analytical integration of Equation 6. It is possible, however, to find an approximation to  $R(\mathbf{k})$  which will be sufficient for our purposes. To ensure overall energy conservation we will be looking for a simple function  $r(\mathbf{k})$  which is bounded by  $R(\mathbf{k})$  from below, i.e.  $R(\mathbf{k}) \leq r(\mathbf{k})$  for any  $\mathbf{k}$ . First of all, we will ignore the loss of energy by the specular component due to the specular lobe going below horizon. This effect is hard to account for for an arbitrary  $n$  and it becomes negligible for large  $n$ , so we will approximate  $R(\mathbf{k})$  as 1 in the absence of Fresnel effects ( $R_s = 1$  in Equation 11). This allows us to write

$$R(\mathbf{k}_1) = \int_{\mathbf{k}_2} f(\mathbf{k}_1, \mathbf{k}_2)(\mathbf{k}_2 \mathbf{n}) F((\mathbf{k} \mathbf{h})) d\omega_{k_2} \leq R_s + (1 - R_s) \int_{\mathbf{k}_2} f(\mathbf{k}_1, \mathbf{k}_2)(\mathbf{k}_2 \mathbf{n}) (1 - (\mathbf{k} \mathbf{h}))^5 d\omega_{k_2}, \quad (13)$$

where  $f(\mathbf{k}_1, \mathbf{k}_2)$  is the part of the specular BRDF without the Fresnel fraction and our approximation says that  $\int_{\mathbf{k}_2} f(\mathbf{k}_1, \mathbf{k}_2)(\mathbf{k}_2 \mathbf{n}) d\omega_{k_2} = 1$ . For a given incident vector  $\mathbf{k}_1$  scalar product  $(\mathbf{k} \mathbf{h})$  is minimal if  $\mathbf{h}$  lies in the plane of incidence and bisects the angle between  $\mathbf{k}_1$  and a vector in  $\mathbf{uv}$  coordinate plane farthest from  $\mathbf{k}_1$ . In this case

$$(\mathbf{k} \mathbf{h})_{min} = \sqrt{\frac{1 - \sqrt{1 - (\mathbf{k}_1 \mathbf{n})^2}}{2}}, \quad (14)$$

and we can choose  $r(\mathbf{k}) = R_s + (1 - R_s)(1 - (\mathbf{k} \mathbf{h})_{min})^5$ . We will further simplify this expression by replacing  $(\mathbf{k} \mathbf{h})_{min}$  with approximation  $(\mathbf{k} \mathbf{h})_{min} \geq (\mathbf{k} \mathbf{n})/2$ . Our approximate hemispherical reflectance becomes

$$r(\mathbf{k}) = R_s + (1 - R_s)(1 - (\mathbf{k} \mathbf{n})/2)^5. \quad (15)$$



**Fig. 4.** Half of a diffusely illuminated sphere with  $R_s = 0.05$  and  $R_d = 1$ . The lowest values are near the edge of the sphere and are approximately 74% of the background.

We can now substitute this as  $R(\mathbf{k})$  into Equation 12 and perform integration to obtain the normalization constant  $c$ . The diffuse term becomes

$$\rho_d(\mathbf{k}_1, \mathbf{k}_2) = \frac{28R_d}{23\pi} (1 - R_s) \left( 1 - \left( 1 - \frac{(\mathbf{n}\mathbf{k}_1)}{2} \right)^5 \right) \left( 1 - \left( 1 - \frac{(\mathbf{n}\mathbf{k}_2)}{2} \right)^5 \right) \quad (16)$$

Note that our diffuse BRDF does not depend on  $n_u$  and  $n_v$ , so we can judge the quality of approximations we made in its derivation by looking at a single image on Figure 2 created in a setting identical to the “furnace” of Figure 4. For large  $n$  there is little loss of energy by the specular term, so any darkening of the sphere is due to the diffuse component.

A set of polished red spheres with different phong exponents  $n_u, n_v$  is shown in Figure 5. For all spheres  $R_s$  is set to 0.05 across the visible spectrum which is a typical value for plastics. In addition to anisotropic highlights and blurred reflections we can observe strengthening of the specular reflection near the silhouette of the sphere along with simultaneous decrease in the intensity of the red color. This effect is more prominent in Figure 6 where three different views of the same scene are shown.

## 4 Implementing the model

Recall the BRDF is a combination of diffuse and specular components:

$$\rho(\mathbf{k}_1, \mathbf{k}_2) = \rho_s(\mathbf{k}_1, \mathbf{k}_2) + \rho_d(\mathbf{k}_1, \mathbf{k}_2). \quad (17)$$

The diffuse component is given in Equation 16. The specular component is given in Equation 10. It is not necessary to call trigonometric functions to compute the exponent, so the specular BRDF is:

$$\rho(\mathbf{k}_1, \mathbf{k}_2) = \frac{\sqrt{(n_u + 1)(n_v + 1)}}{8\pi} \frac{(\mathbf{nh})^{\frac{(n_u(\mathbf{h}\mathbf{u})^2 + n_v(\mathbf{h}\mathbf{v})^2)}{(1 - (\mathbf{h}\mathbf{n})^2)}}}{(\mathbf{hk})\max((\mathbf{n}\mathbf{k}_1), (\mathbf{n}\mathbf{k}_2))} F((\mathbf{k}\mathbf{h})). \quad (18)$$

In a Monte Carlo setting we are interested in the following problem: given  $\mathbf{k}_1$ , generate samples of  $\mathbf{k}_2$  with a distribution which shape is similar to the cosine weighted BRDF. The key part of our thinking on this is inspired by discussion by Zimmerman [12] and



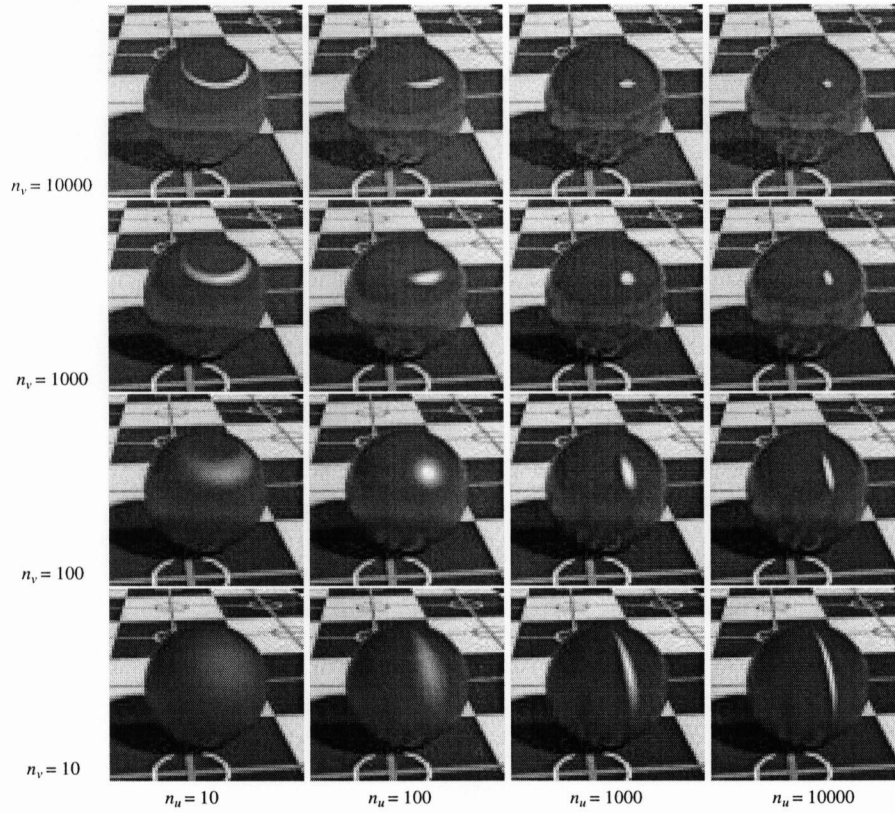


**Fig. 5.** Diffuse spheres for various exponents.

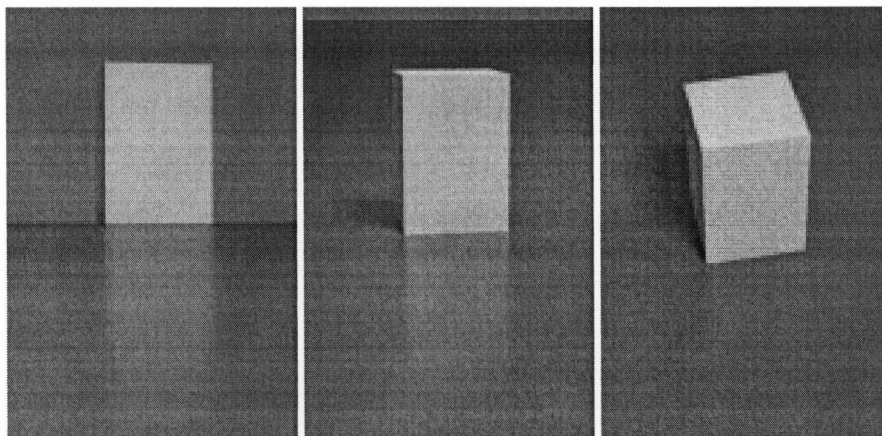


**Fig. 6.** Three views for  $n_u = n_v = 400$  and a red substrate.

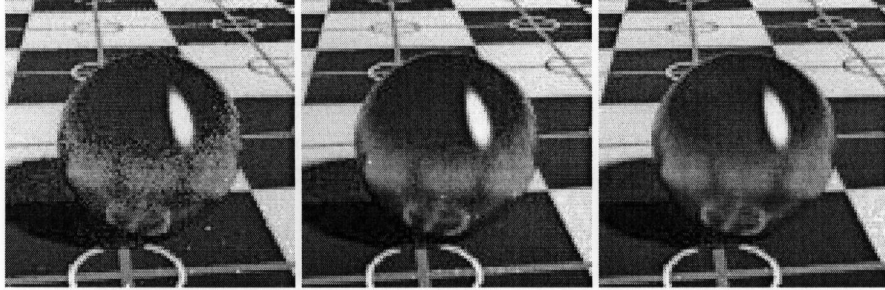


**Fig. 7.** A closeup of the model implemented in a path tracer with 9, 26, and 100 samples.

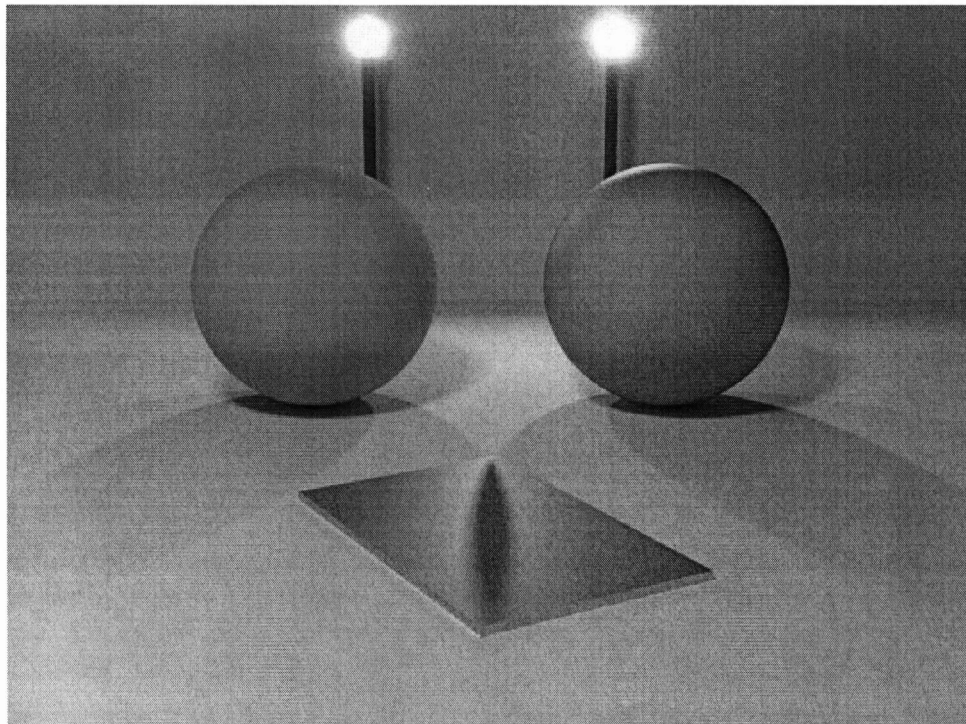


**Fig. 8.** An image with a Lamertian sphere (left) and a sphere with  $n_u = n_v = 5$ .

by Lafortune [4] who point out that greatly undersampling a large value of the integrand is a serious error while greatly oversampling a small value is acceptable in practice. The reader can verify that the densities suggested below have this property.

We can just use the probability density function  $p_h(\mathbf{h})$  of Equation 5 to generate a random  $\mathbf{h}$ . However, to evaluate the rendering equation we need both a reflected vector  $\mathbf{k}_2$  and a probability density function  $p(\mathbf{k}_2)$ . It is important to note that if you generate  $\mathbf{h}$  according to  $p_h(\mathbf{h})$  and then transform to the resulting  $\mathbf{k}_2$ :

$$\mathbf{k}_2 = -\mathbf{k}_1 + 2(\mathbf{k}_1\mathbf{h})\mathbf{h}, \quad (19)$$

the density of the resulting  $\mathbf{k}_2$  is not  $p_h(\mathbf{k}_2)$ . This is because of the difference in measures in  $\mathbf{h}$  and  $\mathbf{v}_2$  space described in Equation 8. So the actual density  $p(\mathbf{k}_2)$  is:

$$p(\mathbf{k}_2) = \frac{p_h(\mathbf{h})}{4(\mathbf{k}_1\mathbf{h})}. \quad (20)$$

Note that it is possible to generate an  $\mathbf{h}$  vector whose corresponding vector  $\mathbf{k}_2$  will point inside the surface, i.e.  $(\mathbf{k}_2\mathbf{n}) < 0$ . The weight of such a sample should be set to zero. This situation corresponds to the specular lobe going below the horizon and is the main source of energy loss in the model. Clearly, this problem becomes progressively less severe as  $n_u, n_v$  become larger.

The only thing left now is to describe how to generate  $\mathbf{h}$  vectors with pdf of Equation 5. We will start by generating  $\mathbf{h}$  with its spherical angles in the range  $(\theta, \phi) \in [0, \frac{\pi}{2}] \times [0, \frac{\pi}{2}]$ . Note that this is only the first quadrant of the hemisphere. Given two random numbers  $(\xi_1, \xi_2)$  uniformly distributed in  $[0, 1]$ , we can choose

$$\phi = \arctan \left( \sqrt{\frac{n_u + 1}{n_v + 1}} \tan \left( \frac{\pi \xi_1}{2} \right) \right), \quad (21)$$

and then use this value of  $\phi$  to obtain  $\theta$  according to

$$\cos \theta = (1 - \xi_2)^{\frac{1}{n_u \cos^2 \phi + n_v \sin^2 \phi + 1}}. \quad (22)$$

To sample the entire hemisphere, the standard manipulation where  $\xi_1$  is mapped to one of four possible functions depending on whether it is in  $[0, 0.25)$ ,  $[0.25, 0.5)$ ,  $[0.5, 0.75)$ , or  $[0.75, 1.0)$ . For example for  $\xi_1 \in [0.25, 0.5)$ , find  $\phi(1 - 4(0.5 - \xi_1))$  via Equation 21, and then “flip” it about the  $\phi = \pi/2$  axis. This ensures full coverage and stratification.

For the diffuse term it would be possible to do importance sample with a density close to cosine-weighted BRDF [16] in a way similar to that described by Shirley et al [10], but we use a simpler approach and generate samples according to cosine distribution. This is sufficiently close to the complete diffuse BRDF to substantially reduce variance of the Monte Carlo estimation.

An example of the model in a full scene inspired by Lafortune [5] is shown in Figure 8. Note the specular effects on the horizon of the right sphere which implements the model of this paper, and the absence of these effects on the left sphere which is Lambertian.

## References

1. James F. Blinn. Models of light reflection for computer synthesized pictures. *Computer Graphics (Proceedings of SIGGRAPH 77)*, 11(2):192–198, July 1977.

2. Robert L. Cook and Kenneth E. Torrance. A reflectance model for computer graphics. *Computer Graphics*, 15(3):307–316, August 1981. ACM Siggraph '81 Conference Proceedings.
3. Donald P. Greenberg, Kenneth E. Torrance, Peter Shirley, James Arvo, James A. Ferwerda, Sumanta Pattanaik, Eric P. F. Lafortune, Bruce Walter, Sing-Choong Foo, and Ben Trumbore. A framework for realistic image synthesis. *Proceedings of SIGGRAPH 97*, pages 477–494, August 1997.
4. Eric P. Lafortune and Yves D. Willems. Using the modified phong BRDF for physically based rendering. Technical Report CW197, Computer Science Department, K.U.Leuven, November 1994.
5. Eric P. F. Lafortune, Sing-Choong Foo, Kenneth E. Torrance, and Donald P. Greenberg. Non-linear approximation of reflectance functions. *Proceedings of SIGGRAPH 97*, pages 117–126, August 1997.
6. Robert Lewis. Making shaders more physically plausible. In Michael F. Cohen, Claude Puech, and Francois Sillion, editors, *Fourth Eurographics Workshop on Rendering*, pages 47–62. Eurographics, June 1993. held in Paris, France, 14–16 June 1993.
7. László Neumann, Attila Neumann, and László Szirmay-Kalos. Compact metallic reflectance models. *Computer Graphics Forum*, 18(13), 1999.
8. Bui-Tuong Phong. Illumination for computer generated images. *Communications of the ACM*, 18(6):311–317, June 1975.
9. Christophe Schlick. An inexpensive BRDF model for physically-based rendering. *Computer Graphics Forum*, 13(3):233–246, 1994.
10. Peter Shirley, Helen Hu, Brian Smits, and Eric Lafortune. A practitioners' assessment of light reflection models. In *Pacific Graphics*, pages 40–49, October 1997.
11. Gregory J. Ward. Measuring and modeling anisotropic reflection. *Computer Graphics*, 26(4):265–272, July 1992. ACM Siggraph '92 Conference Proceedings.
12. Kurt Zimmerman. *Density Prediction for Importance Sampling in Realistic Image Synthesis*. PhD thesis, Indiana University, June 1998.